

Ultrasound critical-angle reflectometry (UCR): a new modality for functional elastometric imaging

Peter Antich and Shreefal Mehta

Advanced Radiological Sciences, Department of Radiology, University of Texas Southwestern Medical Center, 5323 Harry Hines Blvd, Dallas, TX 75235, USA

Received 4 July 1996, in final form 2 April 1997

Abstract. This paper discusses the measurement of velocity in a solid based on the analysis of the amplitude and phase of ultrasound waves reflected by a solid, a technique called ultrasound critical-angle reflectometry (UCR). To this end, the complete formulation of ultrasound wave reflection and refraction from a liquid–solid interface is described. Differences between this formulation and previously published ones are briefly discussed. Based on this analysis it is in particular possible to measure by this technique not only pressure but also, for the first time in such studies, shear wave velocities, an experimentally confirmed result. The measurement of the complete stiffness matrix of a transversely isotropic solid, specifically cortical bone, by applying UCR elastometry to any point on the solid's surface is demonstrated. Finally this method is extended to functional elastometric imaging. The techniques presented in this paper offer new opportunities for applications of UCR imaging to the assessment of bone metabolism, formation and disease and also to the analysis of composite materials in general.

1. Introduction

1.1. Ultrasound measurement of mechanical properties

In a number of conditions, both natural (e.g. aging, osteoporosis) and artificial (e.g. space flight), bone mass has been shown to vary. However, little is known about changes in the intrinsic properties of bone, partially because techniques for measuring specific material and structural properties of bone *in vivo* are not commonly available.

The non-invasive and non-destructive measurement of the intrinsic mechanical properties of bone is possible using ultrasound. The ultrasound velocity, a measurable and well-studied property, is directly related to the elasticity, a quantity which, for bone, not only describes its load-bearing function but also predicts its ultimate (breaking) strength, as has been experimentally shown (Vahey *et al* 1987, Wright *et al* 1987, Turner and Eich 1991, Pak *et al* 1993). The measurement of velocity is therefore clearly relevant to biomedical studies.

The principles of reflection and refraction of ultrasound have been widely applied in fields ranging from the seismological analysis of the composition and structure of subterranean volumes (Mayer 1963) to hurricane detection (Ergin 1952). As discussed below, ultrasound critical-angle reflectometry (UCR) is a specific technique to measure critical angles, which in turn allow a direct measurement of the phase velocity using Snell's law. Most importantly, UCR measures the velocity at any chosen point in the sample without requiring direct contact, and thus is a non-invasive method for measuring not only the velocity but also its distribution and variability along a sample.

1.2. Ultrasound critical-angle reflectometry (UCR): previous studies

An analytical expression for the reflection of ultrasound wavepackets was first derived by Knott in 1899 (Knott 1899). This formulation was subsequently refined for seismological use and for material testing (Blut 1932, Ergin 1952, Brekhovskikh 1960, Mayer 1965, Shutilov 1988) and has been used in materials studies to measure the ultrasound velocity in isotropic materials (Mayer 1963, 1965, Rollins 1965, 1966, 1968, Fountain 1966) and in the study of mineralized tissue *in vitro* (Lees and Rollins 1972, Whiting 1977). These early studies were abandoned as doubts arose about the interpretation of the velocities measured and their relation to transmission (or pulse–echo) velocities. These techniques usually measure velocity from the time-of-flight of an ultrasound pulse over a distance, which in transmission measurements is the distance between two transducers placed at opposite ends of the sample and which in pulse–echo techniques is the distance between a single transducer and the far surface of the sample from which the pulse is reflected back to the transducer (Kaufman and Einhorn 1993).

The interpretive problem is caused by the fact that a critical angle measures the velocity of propagation of the phase of a single-frequency wave, while the transmission (or pulse–echo) technique measures the group velocity, or velocity of transport of energy. When the two velocities are different the medium is dispersive: for a broad range of frequencies, bone has been experimentally shown to be dispersion-free and the two velocities coincide both in cortical and cancellous bone (Lees *et al* 1983, Lakes *et al* 1985). In early studies with the technique developed by us, when the UCR phase velocity was compared directly with a transmission measurement in bovine cortical bone and other laboratory materials, the two were found to be similar for isotropic, homogeneous laboratory materials, and were strongly correlated, but not identical for bone (Antich *et al* 1991b). These differences were attributed not to a dispersive difference between the two velocities, but to the different way in which the two techniques are affected by bone anisotropy, heterogeneity and sample preparation. Further studies have validated the UCR measurement of pressure wave velocity by showing that the elasticity obtained from it is strictly equal to the elasticity measured by mechanical testing for cortical bone (Mehta 1995).

In addition, previous analyses have concentrated on the squared amplitude of the reflected wave alone, which caused discrepancies in interpreting the experimental data, particularly in the measurement of shear wave velocities both for isotropic media and for bone. This problem is addressed below, showing that both the real part of the reflected amplitude and its phase need to be analysed for an accurate measurement of the critical angles.

1.3. Theoretical considerations and methodology

The advantages of the UCR method for clinical studies are considerable. As it analyses the reflected amplitude, it does not require access to bone from two opposing surfaces; as it relies on the measurement of an angle and on the *a priori* measurement of velocity in water only, it does not require an independent measurement of path length. Thus, the technique can be applied both *in vivo* and *in vitro* for the non-invasive and non-destructive study of bone quality (Antich *et al* 1991a,b, Ashman *et al* 1994).

In our laboratory, we developed methodology and instrumentation from an extensive analysis of the phenomenon of ultrasound reflection based on the propagation of ultrasound waves, rather than on the propagation of wavepackets.

We summarize this analysis below and describe its extension to the measurement of a

set of elements of the elasticity matrix at the point studied. In the case of a transversely isotropic material such as bone (Katz and Meunier 1987), this set is complete even when the measurement is made on a single exposed face. The ability to measure multiple elements of the matrix of elasticity and their dependence upon position is essential for ultrasound studies of bone, as this is a composite material in which the material elasticity varies with loading direction (*anisotropy*) and also with location (*heterogeneity*) (Pope and Outwater 1974, Ashman *et al* 1989). Finally, we show that UCR can be developed into a new form of bone imaging, where the image intensity is proportional to elasticity, which can thus be used for inference of resistance to fracture.

In its simplest form, the UCR technique requires the generation of a pure pressure wave in a liquid, e.g. water. Upon arrival at a liquid–solid interface the wave gives rise to a reflected (pressure) wave in the liquid and two refracted (shear and pressure) waves in the solid. The direction of propagation of the incident wave and the normal to the interface define a plane, referred to below as the plane of scattering, which also contains the direction of propagation and particle motion of the reflected and two refracted waves. These are a pressure and shear wave (more generally, a quasi-pressure and quasi-shear wave). A third possible refracted shear wave has particle displacement velocity orthogonal to the plane of scattering (Auld 1973), and thus has zero amplitude as a consequence of continuity.

The amplitude of the reflected wave, measured as a function of the angle (θ) between the incident wave and the normal, is a unique function of the properties of the solid. In particular, it is possible to derive from it the measurement of two *critical* angles, each corresponding to one of the two waves propagating in the solid. A critical angle is the maximum angle of incidence for which the refracted wave can propagate through the solid. In bone, the critical angle corresponding to the pressure wave velocity, θ_1 , is readily observed as it corresponds to total internal reflection in the liquid and to an isolated maximum in the reflected amplitude. The velocity of the pressure wave in the solid is then determined using Snell's law $v = c/\sin\theta_1$. It should be noted that c , the velocity of sound in the liquid, is accurately and precisely known; thus the single measurement of an angle in the liquid is sufficient to obtain an absolute measurement of the velocity in the solid.

Snell's law also applies at the second critical angle, from which the velocity (w) of the shear wave in the solid is obtained as $w = c/\sin\theta_2$. However, this angle is not in general associated with a maximum in the reflected amplitude: to determine its value, the angular dependence of the reflected amplitude must be further analysed. To elucidate this important point, it is necessary to first revisit the theory of wave reflection from a boundary, as described below.

2. Methods

2.1. Theory of UCR analysis

As any ultrasound signal can be considered as the sum of a number of single-frequency plane waves, we consider here for simplicity a single plane wave of angular frequency ω . To further simplify the discussion, we start by considering the problem of reflection from the interface between water and an isotropic solid. When a plane wave travelling through a liquid of density ρ_0 and velocity c impinges, at an angle θ with the normal, upon the surface of an isotropic solid with density ρ , it gives rise to three waves: a pressure wave reflected into the liquid at an angle (ϕ) equal to the angle of incidence (θ), and two refracted waves in the solid (figure 1). These are a pressure wave travelling with velocity v at an angle β , and a transverse (or shear) wave travelling with velocity w at an angle γ .

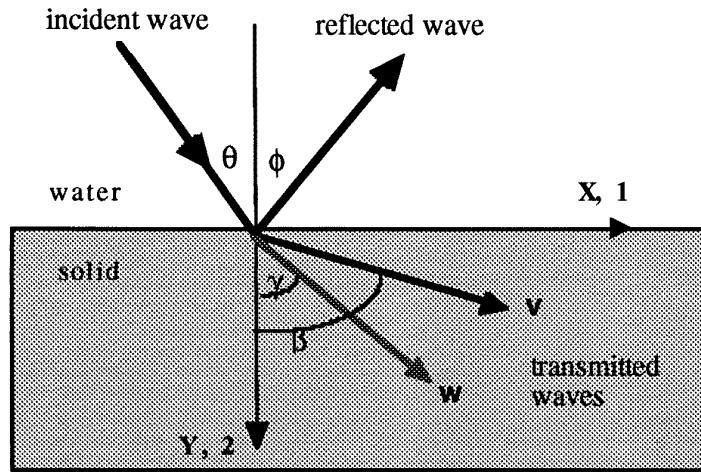


Figure 1. Schematic of reflection and refraction of a plane pressure wave from a liquid–solid interface involving four waves: an incident (I) and reflected (R) pressure wave, one transmitted pressure wave (velocity v) and one transmitted shear wave (velocity w).

A physically relevant description of the ultrasound waves under these conditions is in terms of the displacement velocity \mathbf{U} (the velocity at which particles in the medium are displaced from their equilibrium position; in the following, vector quantities are in bold type). This is because the effect of the wave upon a piezoelectric transducer is proportional to the normal component of \mathbf{U} at its surface.

As stated above, we consider a plane wave incident upon a liquid–solid interface with normal \mathbf{n} . If \mathbf{k}_1 is a unit vector parallel to the direction of propagation of the wave and \mathbf{k}_2 is a unit vector orthogonal to \mathbf{k}_1 in the plane of scattering containing \mathbf{k}_1 and \mathbf{n} , a plane wave in an isotropic medium can be written as

$$\mathbf{U} = \mathbf{k}_1 F_p (\mathbf{r} \cdot \mathbf{k}_1 - vt) + \mathbf{k}_2 F_s (\mathbf{r} \cdot \mathbf{k}_1 - wt) \quad (1)$$

where F_p and F_s are the pressure and shear wave amplitudes with particle motions confined to the plane defined. For waves in a liquid only the first term is non-zero, while both terms exist in a solid.

In a system of coordinates with \mathbf{y} oriented along the normal to the interface and directed into the solid, and \mathbf{x} oriented along the interface (figure 1), the wavevector is written as $\mathbf{k}_1 = \mathbf{y} \cos \theta + \mathbf{x} \sin \theta$ with $\theta < 90^\circ$. It can be seen that displacements and propagation vectors depend only upon two coordinates, x and y . The incident wave (of amplitude normalized to 1,) is represented at a point x, y by (using equation (1)):

$$\mathbf{I} = (\mathbf{x} \sin \theta + \mathbf{y} \cos \theta) \exp[-i\omega(\mathbf{x} \sin \theta + \mathbf{y} \cos \theta - ct)/c]$$

and gives rise to a reflected wave travelling with velocity c at angle ϕ to the normal

$$\mathbf{R} = R(\mathbf{x} \sin \phi - \mathbf{y} \cos \phi) \exp[-i\omega(\mathbf{x} \sin \phi - \mathbf{y} \cos \phi - ct)/c]$$

as well as a refracted pressure wave, travelling with velocity v at angle β to the normal

$$\mathbf{T}_p = T_p(\mathbf{x} \sin \beta + \mathbf{y} \cos \beta) \exp[-i\omega(\mathbf{x} \sin \beta + \mathbf{y} \cos \beta - vt)/v]$$

and a refracted shear wave, travelling with velocity w at angle γ to the normal

$$\mathbf{T}_s = T_s(\mathbf{x} \cos \gamma - \mathbf{y} \sin \gamma) \exp[-i\omega(\mathbf{x} \sin \gamma + \mathbf{y} \cos \gamma - wt)/w].$$

R , T_p , and T_s are the magnitudes of the respective wave amplitudes.

An analytic expression for these amplitudes is obtained by solving the equations derived from the conservation laws which apply at the interface. These imply continuity across the interface of the phases, of the normal components of the displacement velocities and of the stresses, and of energy transfer (Poynting vector), resulting in the following system of equations:

$$\frac{\sin \theta}{c} = \frac{\sin \phi}{c} = \frac{\sin \beta}{v} = \frac{\sin \gamma}{w} \quad (\text{Snell's law}) \quad (2)$$

$$(1 - R) \cos \theta = T_p \cos \beta - T_s \sin \gamma \quad (3)$$

$$\rho c(1 + R) = \rho' v T_p \cos 2\gamma - \rho' w T_s \sin 2\gamma \quad (4)$$

$$\rho' w (T_p \cos \beta \sin \gamma + T_s \cos 2\gamma/2) = 0. \quad (5)$$

Introducing the impedances $Z_0 = \rho c / \cos \theta$, $Z_p = \rho v / \cos \beta$, $Z_s = \rho w / \cos \gamma$, the amplitude of the reflected wave is:

$$R = \frac{Z_p \cos^2 2\gamma + Z_s \sin^2 2\gamma - Z_0}{Z_p \cos^2 2\gamma + Z_s \sin^2 2\gamma + Z_0}. \quad (6)$$

For many isotropic materials and for bone, the velocities v and w are greater than c and therefore there are incidence angles $\theta_1 < 90^\circ$ and $\theta_2 < 90^\circ$ for which $\beta = 90^\circ$ and $\gamma = 90^\circ$ respectively. These are the critical angles for total internal reflection of the pressure and shear waves and divide the region of incidence angles into three parts: region 1, $\theta < \theta_1$; region 2, $\theta_1 < \theta < \theta_2$; and region 3, $\theta_2 < \theta < 90^\circ$.

The solution above only applies in region 1, for as θ exceeds θ_1 , $\sin \beta = (v/c) \sin \theta$ assumes unphysical values greater than 1. At θ_1 , $\cos \beta = 0$, thus Z_p becomes infinite and equation (6) gives $R = 1$. As it is readily seen that a pure (incident) pressure wave cannot give rise to a pure shear wave, a surface pressure wave must be postulated. To investigate the formal nature of such a wave, an analytical continuation to region 2 is readily obtained (Antich 1991a) by setting $\beta = 90 + ib$.

2.1.1. Analytic continuation beyond the first critical angle (region 2). The angle of refraction (β) for the pressure wave, after it reaches 90° , is analytically continued by setting $\beta = 90 + ib$, so that the analytic continuations of $\sin \beta$ and $\cos \beta$ are $\cosh b$ and $-i \sinh b$ respectively. Snell's law can then be rewritten as $\sin \theta / c = \cosh b / v = \sin \gamma / w$. The choice of sign implies that the pressure wave vanishes with increasing depth in the solid as $\exp(-\omega x \sinh b / v)$. The equations relating the amplitudes to each other are then:

$$(1 - R) \cos \theta = -iT_p \sinh b - T_s \sin \gamma \quad (7)$$

$$\rho c(1 + R) = \rho' v T_p \cos 2\gamma - \rho' w T_s \sin 2\gamma \quad (8)$$

$$-iT_p \sinh b \sin \gamma = -T_s \cos 2\gamma/2. \quad (9)$$

From equations (7)–(9), the solution for the real and imaginary part of the reflected amplitude is seen to be

$$\text{Re } R = 1 - 2 \frac{Z_0(Z_0 + Z_s \sin^2 2\gamma)}{Z_p^2 \cos^4 2\gamma + (Z_0 + Z_s \sin^2 2\gamma)^2} \quad (10a)$$

$$\text{Im } R = 2 \frac{Z_0 Z_p \cos^2 2\gamma}{Z_p^2 \cos^4 2\gamma + (Z_0 + Z_s \sin^2 2\gamma)^2}. \quad (10b)$$

We note that the real part of the reflected amplitude describes the response of the receiving transducer, and that at the first critical angle the amplitude is continuous, $\text{Re } R = 1$,

Im $R = 0$. By contrast, at the second critical angle the reflected amplitude has a typically small value given by

$$\operatorname{Re} R = 1 - 2 \frac{Z_0^2}{Z_p^2 + Z_0^2}; \quad \operatorname{Im} R = 2 \frac{Z_0 Z_p}{Z_p^2 + Z_0^2}.$$

2.1.2. *Analytic continuation beyond the second critical angle (region 3).* This second solution is valid until the second critical angle is reached, when γ reaches its limiting value of $\pi/2$. Proceeding as before, Snell's law can be rewritten as

$$\frac{\sin \theta}{c} = \frac{\cosh b}{v} = \frac{\cosh g}{w}.$$

The shear wave has a complex amplitude which vanishes with depth as $\exp(-\omega x \sinh g/w)$. The set of equations (3)–(5) now becomes

$$(1 - R) \cos \phi = -iT_p \sinh b - T_s \cosh g \quad (11)$$

$$Z_0 \cos \phi (1 + R) = -Z_p \sinh b T_p \cosh 2g + iT_s \sinh g T_s \sinh 2g \quad (12)$$

$$iT_p \sinh b \cosh g = -T_s \cosh 2g/2. \quad (13)$$

Solving as before for the real and imaginary parts of the amplitudes, the reflected amplitude is

$$\operatorname{Re} R = 1 - 2 \frac{Z_0^2}{Z_0^2 + (Z_p \cosh^2 2g - Z_s \sinh^2 2g)^2} \quad (14a)$$

$$\operatorname{Im} R = 2 \frac{(Z_p \cosh^2 2g - Z_s \sinh^2 2g) Z_0}{Z_0^2 + (Z_p \cosh^2 2g - Z_s \sinh^2 2g)^2}. \quad (14b)$$

At the second critical angle the new amplitude is continuous with that given by equations (10a) and (10b).

In all regions, solutions for the amplitudes of the refracted waves (T_p and T_s) can also be derived to offer a complete description of the reflection and transmission of sound waves in the two media.

2.2. Experimental set-up for UCR measurements

In UCR, changes in the amplitude and phase of an ultrasound beam reflected from a bone/soft tissue interface are analysed at a constant distance from the point at which reflection occurs over a range of incidence angles, in the plane defined by the direction of the incident beam and the normal to the interface, to obtain the pressure and shear wave velocities in the solid as described earlier. A device built to operate on these principles is briefly described below (Antich *et al* 1991b, Mehta 1995).

Two pressure-wave transducers (Panametrics, Waltham, MA, 5 MHz, planar, 0.373" and 0.5" diameter), a transmitter and a receiver, are mounted on arms that rotate about a centre where a sample is mounted, coplanar with and facing the transducers. Computer-controlled stepper motors (Superior Electric, Bristol, CT, model M061-LS02), move the transducer arms (angular resolution $\sim 0.3^\circ/\text{step}$). An ultrasound pulse of four cycles, generated by a Tektronix (Beaverton, OR) AFG-5101 signal generator at 5 MHz, is reflected off the face of the sample and reaches the receiving transducer, positioned at the same angle from the normal of the sample surface as is the transmitter. The determination of the normal of the material surface must be carefully performed for subsequent accurate measurement of the critical angles. As the transducers are moved synchronously apart, the entire waveform,

sampled and stored using a digital storage oscilloscope (Tektronix 2430A), is processed at each step to obtain the reflected amplitude and phase spectra. A demodulated, amplified return signal can be simultaneously digitized by an A/D converter (DAS-16F, Keithley Metrabyte, Cleveland, OH) over a user-defined time interval for measurement of the reflected amplitude alone.

The bone samples used in this study were cut from the diaphysis of a bovine femur, with the z (3) axis parallel to the long axis of the bone and the 2 axis along the tangential direction chosen to match the coordinate system of previous studies of bone elasticity (Yoon and Katz 1976, Van Buskirk and Ashman 1981a, Ashman *et al* 1984, Katz and Yoon 1984, Kim and Walsh 1993).

3. Results—simulations and experimental data

Phase and amplitude spectra from a cortical bone sample were obtained experimentally (Antich *et al* 1991b, Mehta 1995) as described above and a numerical simulation of equations (6), (10a, b) and (14a, b) was obtained using values chosen to match the experimental data $v \sim 3315 \text{ m s}^{-1}$, $w \sim 1790 \text{ m s}^{-1}$ and $c = 1500 \text{ m s}^{-1}$. The angular dependence of the amplitude and phase of the received signal match the theoretical expectations (figures 2 and 3).



Figure 2. Experimental data (full curve) and theoretical simulation (broken curve) for the amplitude of the pressure wave reflected from cortical bone. The pronounced peak in the amplitude spectrum, followed by the abrupt drop, allows the determination of the pressure critical angle (arrow; pressure wave internally reflected). From this angle and the ultrasound velocity in water, known with high precision and accuracy, the pressure wave in the solid is obtained by Snell's law. By contrast, no pronounced peak is observed in correspondence to the shear wave critical angle. A chi-squared fit between these two spectra gave a probability of 1 (degrees of freedom = 125).

The critical angle (θ_1) for total internal reflection of the pressure wave is obtained by measuring the angle of incidence where the real part of the reflected amplitude is greatest (arrow in figure 2). This peak is followed by an abrupt drop in amplitude. In contrast,

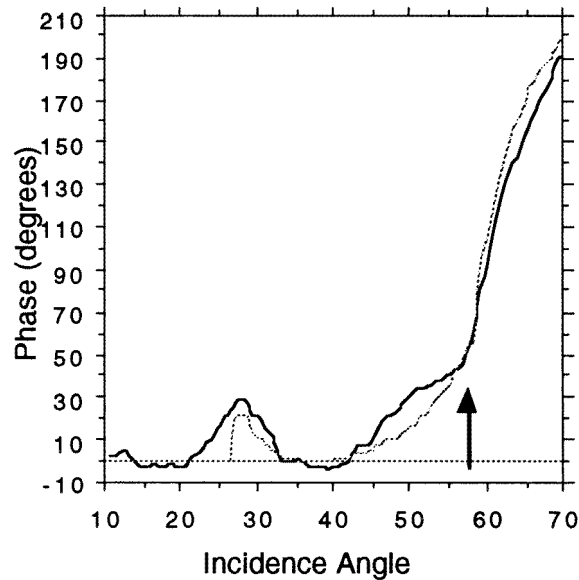


Figure 3. Experimental data (full curve) and theoretical simulation (broken curve) of variations in the phase of the pressure wave reflected from cortical bone are shown in this figure. The sharp change in the slope of the phase spectrum (arrow; shear wave internally reflected), followed by the abrupt rise through 90° , allows the determination of the shear critical angle. The shear wave velocity in bone is determined from this angle and the ultrasound velocity in water, using Snell's law as before. A chi-squared test showed no difference between the two spectra (chi-statistic = 48.52, $\nu = 101$; angles 10° – 60° ; probability = 1).

the critical angle (θ_2) for the shear wave in bone is not easily discerned in the received amplitude spectrum. However, the slope of the phase spectrum shows a distinct change in behaviour at this point (arrow in figure 3), as it varies slowly before this angle, but rises rapidly after it to pass through a 90° phaseshift corresponding to the minimum in the amplitude.

The shear velocities measured in a variety of materials (isotropic metals and cortical bone samples) using UCR and transmission techniques are similar (Mehta and Antich 1997) (with the linear regression fit having a slope of 1), validating experimentally the analytic formulation presented here.

4. UCR elastometry—measurement of elasticity matrix

As described in the previous section, the pressure and shear wave velocities are obtained at a particular point on a sample, in the plane defined by the incident wave and the normal of the interface. By rotating this plane (by angle ψ) around the normal (figure 4), a complete angular distribution of the velocities at that point can be obtained. This change in the velocity with direction is particularly strong in composite materials such as bone and is shown in figure 5(a), (b).

The velocity (V) at a particular orientation is related to the elasticity or material stiffness constant (c_{IJ}) in that plane, and the density (ρ) as $V^2 = c_{IJ}/\rho$. The constants c_{IJ} are identified by so-called 'abbreviated' indices $I, J = 1$ – 6 each of which represent a pair of Cartesian indices: $I = 1$ corresponds to $i, j = 1, 1$; 2 to the pair 2,2; 3 to 3,3; 4 to 2,3; 5

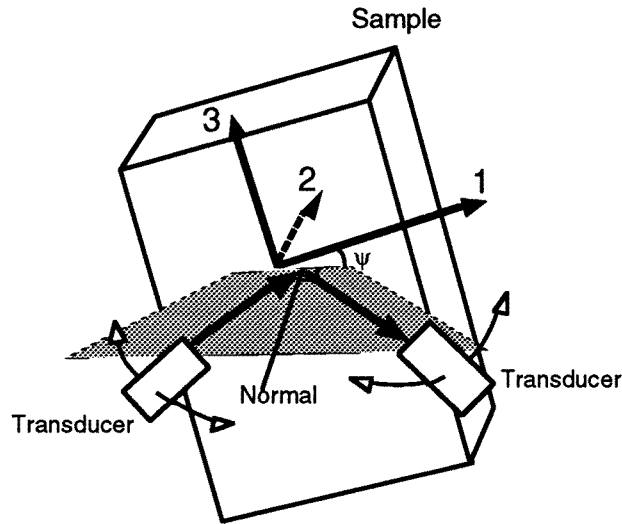


Figure 4. Schematic showing the plane of velocity measurements as defined by the transducers and the normal to the specimen. The velocity measurements of the material are made in this plane of scattering. By rotating the sample or the transducers around the normal axis (orientation angle ψ), this plane of scattering is rotated and an angular distribution of the velocities can be obtained. A chi-squared test showed no difference between the two spectra (chi-statistic = 52.4, $\nu = 131$; angles 10° – 70° ; probability = 1).

to 1,3; 6 to 1,2. The pressure and shear velocities are measured at each orientation step in the rotated plane of scattering.

Cortical Haversian bone is a transversely isotropic material with symmetry in elasticities in the plane normal to the long axis of the bone (Katz and Meunier 1987). The matrix of elasticity (stiffness) is completely defined by five independent coefficients, c_{11} , c_{33} , c_{12} , c_{13} and c_{44} as shown here

$$[c]_{\text{isotropy}}^{\text{transverse}} = \begin{bmatrix} c_{11} & c_{12} & c_{13} & 0 & 0 & 0 \\ c_{12} & c_{11} & c_{13} & 0 & 0 & 0 \\ c_{13} & c_{13} & c_{33} & 0 & 0 & 0 \\ 0 & 0 & 0 & c_{44} & 0 & 0 \\ 0 & 0 & 0 & 0 & c_{44} & 0 \\ 0 & 0 & 0 & 0 & 0 & c_{66} \end{bmatrix} \quad \text{where } c_{66} = \frac{c_{11} - c_{12}}{2}$$

Rotating the sample around its normal by an angle (ψ = the angle by which the plane of measurement is rotated), the square of the velocities in this plane, are expressed in terms of the rotated stiffness coefficients and the density

$$v^2(\psi) = c'_{33}/\rho \quad w^2(\psi) = c'_{44}/\rho. \tag{15}$$

Here, ψ is zero when oriented along the length of the bone (3 axis, 3–2 plane) and 90° along the breadth (1 axis, 1–2 plane) of the bone sample as shown in figure 4. The rotated stiffness coefficients are obtained by applying the Bond transformation (Auld 1973) to the stiffness matrix, for a rotation of ψ around the x axis:

$$c'_{33} = \cos^4(\psi)c_{33} + \sin^4(\psi)c_{11} + 2 \cos^2(\psi) \sin^2(\psi)(c_{13} + 2c_{44}) \tag{16}$$

and similarly, with particle motion in 1–2, 3–2 planes at $\psi = 90^\circ$, $\psi = 0^\circ$ respectively

$$c'_{44} = \cos^2(\psi)c_{44} + \sin^2(\psi)c_{66}. \tag{17}$$

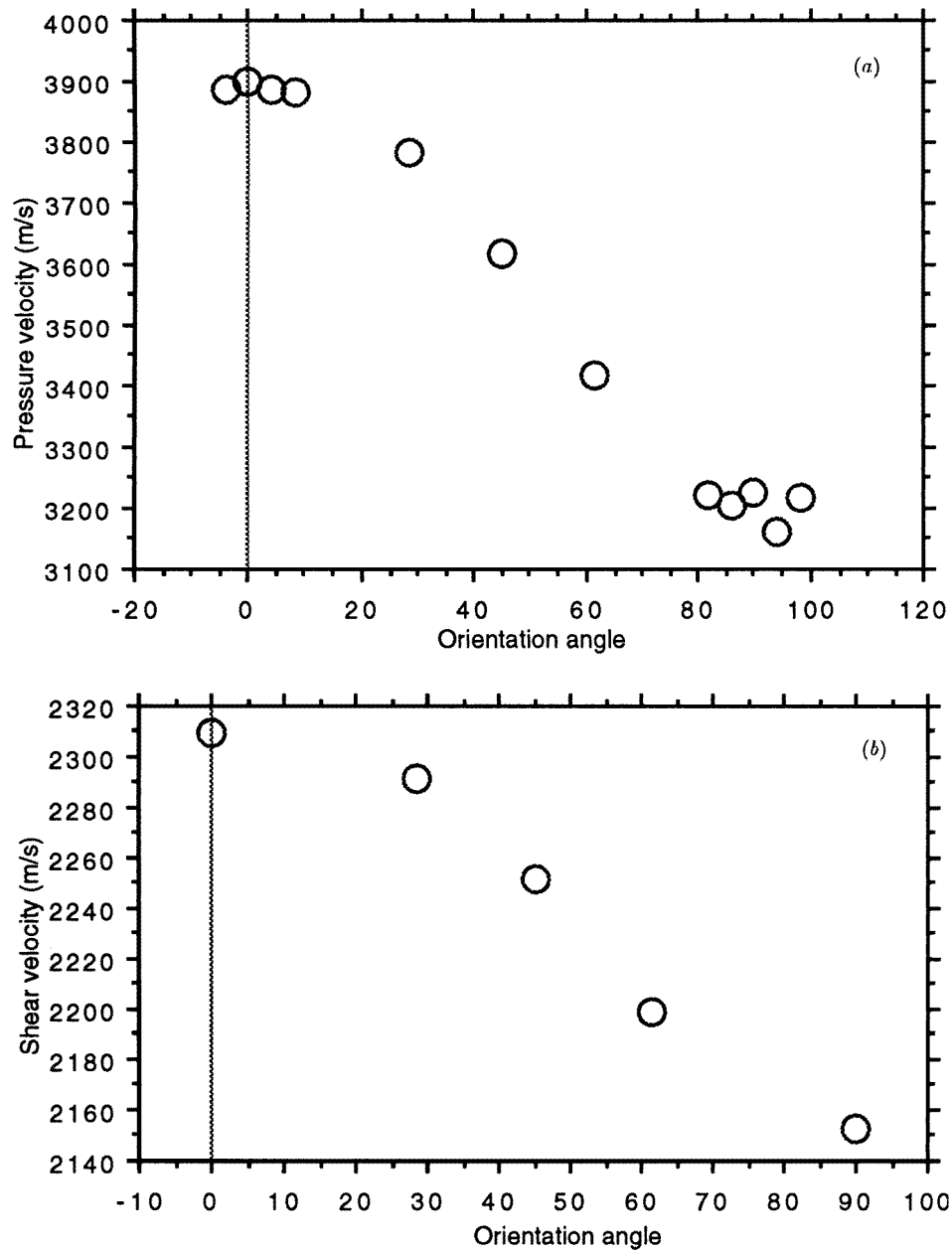


Figure 5. Anisotropy of (a) pressure and (b) shear wave velocities in a sample specimen of cortical bovine bone. Distribution of velocities over a 90° rotation of the plane of measurement are shown here.

The set of equations (15)–(17) defines the relation between the velocity distribution and the principal elasticity coefficients and can be solved to give the five elasticity coefficients. By plotting the square of the pressure and shear wave velocities against the $\cos^2(\psi)$ function as the plane of measurement is rotated around the normal (figure 6), an excellent least-squares

quadratic fit (coefficient of correlation $R^2 = 0.99$) is obtained to the experimental data, indicating that the theoretical assumptions are in conjunction with the anisotropy of bone material properties. Using equations (16) and (17) it can be seen that measurement of the two critical angles at a number of angles ψ , is sufficient to give us a solution for the five elasticity coefficients from these fitted curves. All five coefficients of the stiffness matrix at a specific location are thus obtained from a single surface of the bone using the UCR technique.

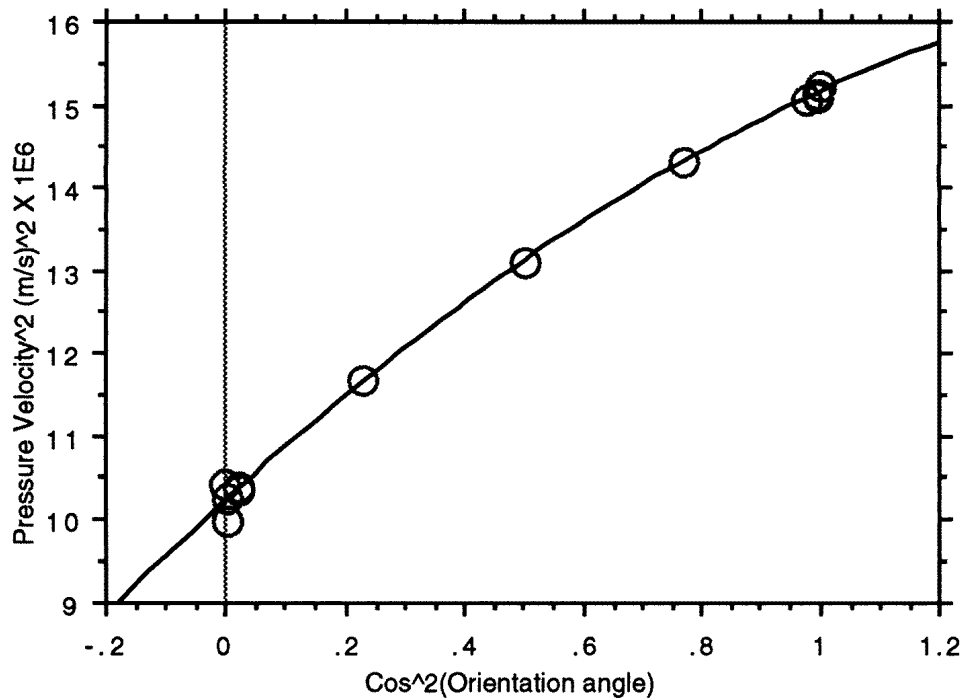


Figure 6. Pressure wave velocity from figure 5(a), fitted to the \cos^2 function of the rotation angle (ψ), as per equation (16). The correlation coefficient (R^2) of the quadratic fit is 0.997. The coefficients of this fitted curve are used to obtain the elasticity coefficients.

Average values for individual components of the stiffness matrix obtained from UCR analysis of a large number of bovine cortical samples, are shown to be within the range of values reported by other researchers (table 1) who have used the transmission technique (Lang 1970, Van Buskirk *et al* 1981b, Katz and Yoon 1984, Kim and Walsh 1993). The variations in this dataset reflect the intrinsic heterogeneity and site dependence of bone material properties. These variations of individual components are indicative of bone structural adaptation and measurement of these components over a region of interest using UCR elastometry has the potential to greatly enhance our understanding of the structure–function relationship in bone. The technique of UCR elastometry imaging is demonstrated in the following section, providing a comprehensive and powerful tool for analysis of bone properties.

Table 1. Averages of elasticity coefficients obtained by the various ultrasound techniques compared. All previous studies used transmission ultrasound measurements with elaborate sample preparation techniques to obtain the required velocity and elasticity measurements. The UCR technique was used to make measurements of pressure and shear velocity anisotropy at a few locations on a large number of bone samples. These readings were used to obtain the elasticity matrices for individual samples and the means of these readings are shown here in the column titled 'This study'. The relative relationships between the individual elasticity components of bone material are maintained and the absolute values are in the range of those reported in the other columns.

Coefficients (GPa)	Lang (1970)	Van Buskirk <i>et al</i> (1981)	Katz <i>et al</i> (1984)	Kim <i>et al</i> (1992)	This study
c_{11}	19.7	16.25	22.4	24.4	27.19
c_{33}	32.0	25.00	25.0	37.6	36.36
c_{44}	5.4	6.65	8.2	10.2	9.02
c_{12}	12.1	6.34	14.0	14.9	12.23
c_{13}	12.6	5.89	13.6	9.5	13.20
c_{66}	3.8	4.96	6.1	9.2	7.47

5. Functional imaging with UCR

The local measurement of material elasticity with UCR makes it possible to generate images by moving the point of measurement around the surface and taking anisotropy measurements at each location. These measurements can then be represented on a colour scale. The directional dependence of the velocity at a set of points (~ 1 mm apart) on a small machined sample of bovine cortical bone (10×7 mm) is shown in a series of five images, the first showing the velocities measured parallel to the sample's lengthwise axis (rotation 0°), then next at rotations of 30° , 45° , 60° and 90° (transverse direction) to this axis (figure 7). The 3, 2 and 1 orthogonal axes (figure 4) were aligned along the length, the radius and the breadth (tangential to surface) respectively, of the cylindrical diaphysis of the long bone from which the sample was cut.

The stiffness matrix obtained at each point using equations (16) and (17) was inverted to give the compliance matrix, from which the technical constants of elasticity, i.e. the principal and shear elastic moduli and the Poisson's ratios, were obtained (Ashman *et al* 1984, Mehta 1995). Variations in the principal elastic moduli, E_1 and E_3 , (Young's moduli along the transverse (1) and long (3) bone axes respectively) are mapped over the sample space (4×7 mm) (figure 8).

These images demonstrate the use of the UCR elastometry technique for measurement of properties of changes in bone status. Thus, changes in the lines of principal stress at a bone site *in vivo* could be followed with time to infer changes in the functional response and the metabolic status of the bone. The UCR technique has been used in the clinic for measurement of pressure velocities (Antich *et al* 1993) and bone anisotropy *in vivo*. Further studies are in progress to expand the *in vivo* imaging capabilities of this technique by adding the measurement of shear velocity and corrections for propagation of ultrasound waves in soft tissue.

6. Summary

In summary, we have discussed the theory governing the reflection of ultrasound at liquid–solid boundaries. We note that this theory has applications in a variety of areas from

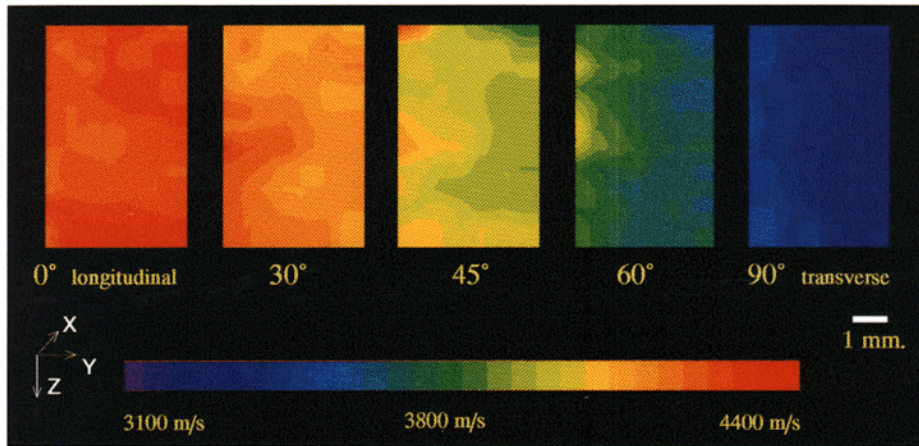


Figure 7. Heterogeneity of bone material: Images of angular dependence of bone velocity at $\psi = 90^\circ, 60^\circ, 45^\circ, 30^\circ, 0^\circ$ rotation of scattering plane at a point in a sample.

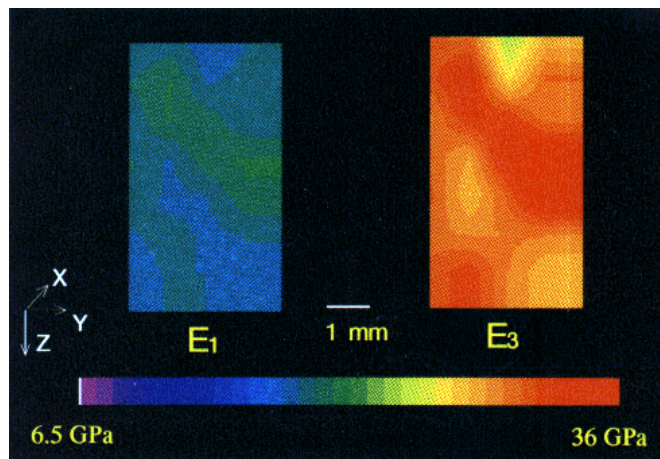


Figure 8. Heterogeneity of Young's moduli and bone material: E_3 (along long axis of bone) and E_1 (along transverse axis of bone). These elasticity constants are derived by inversion of the stiffness matrix obtained using equations (16) and (17).

geophysics to medicine (Brekhovskikh 1960). As the most general ultrasound beam can be described as a superposition of partial waves, we have discussed a plane-wave formulation of the theory, and we have demonstrated that a simple technique (UCR) can be implemented to measure both pressure and shear wave velocity as well as their anisotropy in bone material, both in the laboratory and in the clinic. From such measurements, we have shown that the complete transverse isotropy stiffness matrix can be obtained from a single surface of bone, and that consequently a complete description of Haversian bone material can be derived at any point in bone. This property makes it possible to obtain images of the elasticity matrix of bone, presented here for the first time. As in other applications, this extension to imaging permits an evaluation not only of the numerical values of the elasticity but also of its distribution and variability. These properties appear *a priori* necessary for a full understanding of the biomechanical properties of bone.

References

- Antich P, Anderson J, Ashman R, Dowdey J, Gonzales J, Murry R, Zerwekh J and Pak C 1991b Measurement of mechanical properties of bone material in vitro by ultrasound reflection: methodology and comparison with ultrasound transmission *J. Bone Miner. Res.* **6** 417–26
- Antich P, Dowdey E and Murry R C 1991a Method and apparatus for analyzing material properties using reflected ultrasound *US Patent* 5 038 787
- Antich P, Pak C, Gonzales J, Anderson J, Sakhaee K and Rubin C 1993 Measurement of intrinsic bone quality in vivo by reflection ultrasound: Correction of impaired quality with slow-release sodium fluoride and calcium citrate *J. Bone Miner. Res.* **8** 301–11
- Ashman R, Antich P, Gonzales J, Anderson J and Rho J 1994 A comparison of reflection and transmission ultrasonic techniques for measurement of cancellous bone elasticity *J. Biomech.* **27** 1195–9
- Ashman R, Cowin S, Van Buskirk W and Rice J 1984 A continuous wave technique for the measurement of the elastic properties of cortical bone *J. Biomech.* **17** 349–61
- Ashman R, Rho J and Turner C 1989 Anatomical variation of orthotropic elastic moduli of the proximal human tibia *J. Biomech.* **22** 895–900
- Auld B 1973 *Acoustic Fields and Waves in Solids* vol 1 (New York: Wiley)
- Blut H 1932 V. Ein Beitrag zur Theorie der Reflexion und Brechung elastischer Wellen an Unstetigkeitsflächen *Z. Geophys.* **8** 130–44
- Brekhovskikh L 1960 *Waves in Layered Media* (New York: Academic)
- Ergin K 1952 Energy ratio of the seismic waves reflected and refracted from a rock-water boundary *Bull. Seismol. Soc. Am.* **42** 349–72
- Fountain L S 1966 Experimental evaluation of the total reflection method of determining ultrasonic velocity *J. Acoust. Soc. Am.* **42** 242–7
- Kaufman J and T Einhorn 1993 Perspectives: ultrasound assessment of bone *J. Bone Miner. Res.* **8** 517–25
- Katz J and Meunier A 1987 The elastic anisotropy of bone *J. Biomech.* **20** 1063–70
- Katz J and Yoon H 1984 The structure and anisotropic mechanical properties of bone *IEEE Trans. Biomed. Eng.* **31** 878–84
- Kim H and Walsh W 1993 Mechanical and ultrasonic characterization of cortical bone *Biomimetics* **1** 293–370
- Knott C 1899 Reflexion and refraction of elastic waves with seismological applications *Phil. Mag.* **48** 64
- Lakes R, Yoon H and Katz J 1985 Ultrasonic wave propagation and attenuation in wet bone *J. Biomed. Eng.* **8** 143–8
- Lang S 1970 Ultrasonic method for measuring elastic coefficients of bone and results of fresh and dried bones *IEEE Trans. Biomed. Eng.* **17** 101–5
- Lees S, Ahern J and Leonard M 1983 Parameters influencing the sonic velocity in compact calcified tissues of various species *J. Acoust. Soc. Am.* **74** 28–33
- Lees S and Rollins F 1972 Anisotropy in hard dental tissues *J. Biomech.* **5** 557–66
- Mayer W 1963 Reflection and refraction of mechanical waves at solid-liquid boundaries *J. Appl. Phys.* **34** 909–11
- 1965 Energy partition of ultrasonic waves at flat boundaries *Ultrasonics* **3** 62–8
- Mehta S 1995 Analysis of mechanical properties of bone material using nondestructive ultrasound reflectometry *PhD Thesis* University of Texas Southwestern Medical Center
- Mehta S and Antich P 1997 Measurement of shear-wave velocity by ultrasound critical-angle reflectometry (UCR) *Ultrasound Med. Biol.* at press
- Pak C, Sakhaee K, Antich P, Zerwekh J, Peterson R, Piziak V, Gonzales J, Hatab M and Poindexter J 1993 Update on the treatment of osteoporosis with intermittent slow release sodium fluoride and continuous calcium chloride *Proc. 4th Int. Symp. on Osteoporosis (Aalborg, Denmark)* ed C Christiansen and B Riis (Rodovre: Osteopress) pp 122–4
- Pope M and Outwater J 1974 Mechanical properties of bone as a function of position and orientation *J. Biomech.* **7** 61–6
- Rollins F 1965 Ultrasonic reflectivity at a liquid–solid interface near the angle of incidence for total reflection *Appl. Phys. Lett.* **7** 212–4
- 1966 Critical ultrasonic reflectivity—a neglected tool for material evaluation *Mater. Eval.* **24** 683–9
- 1968 Ultrasonic examination of liquid–solid boundaries using a right-angle reflector technique *J. Acoust. Soc. Am.* **44** 431–4
- Shutilov V 1988 *Fundamental Physics of Ultrasound* (New York: Gordon and Breach)
- Turner C and Eich M 1991 Ultrasonic velocity as a predictor of strength in bovine cancellous bone *Calcif. Tissue Int.* **49** 116–19
- Vahey J, Lewis J and Vanderby R 1987 Elastic moduli, yield stress, and ultimate stress of cancellous bone from the proximal tibial epiphysis *J. Biomech.* **20** 29–33

- Van Buskirk W and Ashman R 1981a The elastic moduli of bone *Mechanical Properties of Bone* ed S Cowin (Colorado: American Society of Mechanical Engineers) pp 131–43
- Van Buskirk W, Cowin S and Ward R 1981b Ultrasonic measurement of orthotropic elastic constants of bovine femoral bone *J. Biomech. Eng.* **103** 67–72
- Whiting J 1977 Ultrasound critical angle reflection goniometer for in vivo bone mineral analysis *Ultrasound in Medicine* ed D White and R Brown (New York: Plenum) pp 1629–43
- Wright L, Glade M and Gopal J 1987 The use of transmission ultrasound to assess bone status in the human newborn *Pediatric Res.* **22** 541–4
- Yoon H S and Katz J L 1976 Ultrasonic wave propagation in human cortical bone-II. Measurements of elastic properties and hardness *J. Biomech.* **9** 459–64